Electro-acoustic component placement optimization for helicopter cabin ANC systems

Yuhang Yang*, Liquan Shi*, Ningyuan liang† and Guoyong Jin*
* Harbin Engineering University, Harbin 150001, China
† Heilongjiang Provincial Key Laboratory of Aerodynamic Noise and Control
China Aerodynamics Research and Development Center, Harbin 150001, China
E-mail: guoyongjin@hrbeu.edu.cn

***Abstract*—This paper investigates the optimization of electro-acoustic component placement in helicopter cabin active noise control (ANC) systems using the θ-Non-dominated Sorting Genetic Algorithm III (θ-NSGA-III). The acoustic transfer impedance matrixes of the ANC system were obtained through numerical simulation, with electro-acoustic components modeled as discrete nodes. The continuous optimization problem of component placement was transformed into a discrete optimization task. Aiming to minimize the sum of squared sound pressures at measurement points near the occupant's head, multiple independent runs of the θ-NSGA-III algorithm yielded an optimal configuration for electro-acoustic component placement. Experimental comparison with the conventional scheme confirmed that the optimized configuration significantly enhanced the noise reduction performance of the helicopter cabin ANC system.**

I. INTRODUCTION

Cabin noise in helicopters significantly impacts both the physical and psychological well-being of occupants and the stable operation of onboard equipment, making its control an essential area of research[1]. Active noise control (ANC) technology, known for its adaptability to complex operational conditions and excellent broadB(A)nd noise reduction performance, is an important approach for noise control within enclosed cabin spaces[2].

The spatial layout and quantity of electro-acoustic components in helicopter cabin ANC systems play a critical role in determining noise reduction performance[3]. However, the optimization of such systems remains challenging, as it involves multiple interdependent factors and constitutes a complex multi-objective optimization problem[4]. Traditionally, heuristic optimization methods have been widely utilized and have yielded noteworthy results[5]. For instance, Baek et al[6]. employed genetic algorithms in rectangular-space ANC system design, constructing multi-objective optimization models to balance the number and configuration of secondary sources and error sensors against noise reduction performance. Wang et al[7]. proposed a novel progressive search approximation strategy based on a genetic algorithm, which alternates between fixed and flexible parameter optimization. This method accounts for the interdependence among parameters such as the positions and intensities of secondary sources. Additionally, optimization research specifically targeting ANC device layouts within complex enclosed spaces, such as helicopter cabins, remains relatively sparse, highlighting the need for more efficient optimization methodologies.

This paper presents an optimization strategy for the spatial layout of electro-acoustic components in helicopter cabin ANC systems based on the θ-NSGA-III[8]. By discretizing the acoustic field within the enclosed cabin, the continuous optimization problem of component placement was transformed into a discrete combinatorial optimization task. The objective function is defined as the minimization of the sum of squared sound pressures at measurement points, from which the optimal configuration is derived using the θ-NSGA-III algorithm. Experimental validation demonstrates that the ANC system with the optimized configuration achieves up to 21.4 dB of global noise reduction at occupant head height within the 20–500 Hz frequency range—representing an improvement of 5.1 dB over the conventional configuration.

II. THEORETICAL MODELING OF ACTIVE NOISE CONTROL FOR CABIN NOISE

The expression for the sound pressure at an arbitrary error sensor e within the enclosed helicopter cabin is given by:

$$p_e = p_p + p_s \tag{1}$$

where, p_e denotes the acoustic pressure at the error sensor e; p_p represents the acoustic pressure at measurement point e induced by the primary noise source; and p_s denotes the acoustic pressure at measurement point e generated by the secondary source. Further, the acoustic pressures at measurement point e arising from the primary and secondary sources can be expressed as follows:

$$p_p = \boldsymbol{Z}_p \boldsymbol{q}_p,\ p_s = \boldsymbol{Z}_s \boldsymbol{q}_s \tag{2}$$

979-8-3315-7206-8/25/$31.00 ©2025 IEEE

where $\boldsymbol{Z}_p$ and $\boldsymbol{Z}_s$ denote the acoustic transfer impedance matrices composed of transfer functions from the primary and secondary sources to the error sensor e, respectively. Meanwhile, $\boldsymbol{q}_p$ and $\boldsymbol{q}_s$ represent the acoustic source strength vectors of the primary and secondary sources, respectively.

To achieve noise reduction within the targeted quiet zone of an enclosed cabin, the theoretical control objective is to minimize the total radiated acoustic power from both primary and secondary sources. Under the assumption that all error sensors used possess identical frequency responses and sensitivities, minimizing the total acoustic power is theoretically equivalent to minimizing the sum of squared sound pressures at each error sensor[3]. Furthermore, the sum of squared sound pressures is mathematically simpler to handle, thus facilitating rapid convergence and enhanced computational efficiency of optimization algorithms. Accordingly, considering M error sensors, the objective function for minimizing the sum of squared sound pressures at these points is defined as:

$$\boldsymbol{J}_e = \sum_{i=1}^{M} \left| p_{e,i} \right|^2 \tag{3}$$

where M denotes the number of error sensors. By substituting Eq.(1) and (2) into Eq.(3), the expanded form of the objective function is obtained as follows:

$$\boldsymbol{J}_e = \boldsymbol{P}_e^H \boldsymbol{P}_e = (\boldsymbol{Z}_p \boldsymbol{q}_p + \boldsymbol{Z}_s \boldsymbol{q}_s)^H (\boldsymbol{Z}_p \boldsymbol{q}_p + \boldsymbol{Z}_s \boldsymbol{q}_s) \tag{4}$$

where $\boldsymbol{P}_e=[p_{e,1}\ p_{e,2}\ \dots\ p_{e,3}]^{\mathrm{T}}$ denotes the column vector of sound pressures of M measurement points.

By taking the partial derivative of $\boldsymbol{J}_e$ with respect to $\boldsymbol{q}_s$ and setting it to zero, the optimal secondary source strength vector $\boldsymbol{q}_s$ can be obtained under the condition that the primary source strength $\boldsymbol{q}_p$ is known:

$$\boldsymbol{q}_s = -(\boldsymbol{Z}_s^H \boldsymbol{Z}_s)^{-1} \boldsymbol{Z}_s^H \boldsymbol{Z}_p \boldsymbol{q}_p \tag{5}$$

where H denotes the Hermitian (conjugate transpose) operator.

To evaluate the noise reduction effectiveness at the target zone after incorporating the secondary source array, and to assess the performance of different configuration schemes, the noise reduction level at the i-th evaluation point and the global noise reduction level of the ANC system are defined as L_i and T, respectively. Their corresponding expressions are given by:

$$\begin{aligned} L_i &= -20\log_{10}\left(\frac{|p_{c,i}|}{|p_{woc,i}|}\right) \\ T &= 10\log_{10}\left(\frac{1}{N}\sum_{i=1}^{N} 10^{\frac{L_i}{10}}\right) \end{aligned} \tag{6}$$

where $p_{woc,i}$ and $p_{c,i}$ denote the sound pressures at the i-th evaluation point before and after the introduction of secondary sources, respectively, and N represents the total number of evaluation points.

III. Computation of the Acoustic Transfer Impedance Matrix

The acoustic transfer impedance matrix constitutes a critical component in the simulation of the ANC system. Given the large number of parameters and operating conditions involved in the optimization process, a numerical simulation model of the cabin section was established in *Virtual.Lab* to obtain the acoustic transfer impedance matrices required for control system modeling. The numerical model of the helicopter cabin used for simulation is illustrated in Fig. 1. The white dots distributed around the periphery of the helicopter cabin represent the simulated primary sound sources. In the simulation, the primary source points are excited using noise recordings captured during actual helicopter operation. Based on this excitation, the acoustic transfer impedance matrix for the primary noise field is obtained.

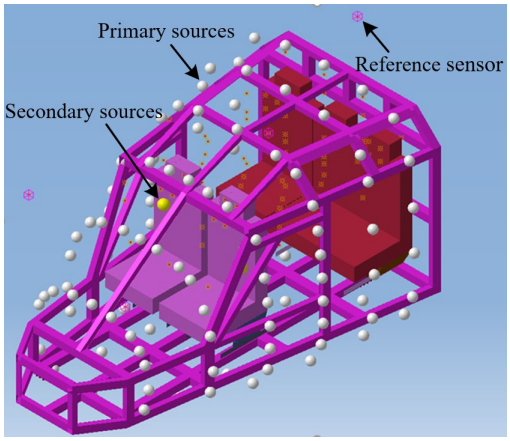

Fig. 1 Numerical Simulation Model of the Helicopter Cabin

The potential placement region for secondary sources in the helicopter cabin is further abstracted and simplified as a closed rectangular cavity with dimensions of 1.8 m×1.6 m×1.35 m, as illustrated in Fig. 2. The medium inside the cavity is assumed to be air, with a sound speed of c=343m/s and a density of ρ=1.29kg/m^3. All six internal boundaries of the cavity are modeled as uniformly low-damping walls. The target frequency range for noise control is set between 20 Hz and 500 Hz, corresponding to a minimum acoustic wavelength of $\lambda_{\min}=c/f_{\text{high}}=0.686m$.

To facilitate the application of multi-objective evolutionary algorithms in solving the optimization problem of the cabin ANC system, all sound sources within the space are assumed to be point sources. The cabin interior is discretized by appropriate grid partitioning, and the candidate coordinates for electro-acoustic components are constrained to a finite set of grid nodes within the cabin. This transforms the continuous-domain optimization problem of the ANC system into a discrete-domain optimization problem.

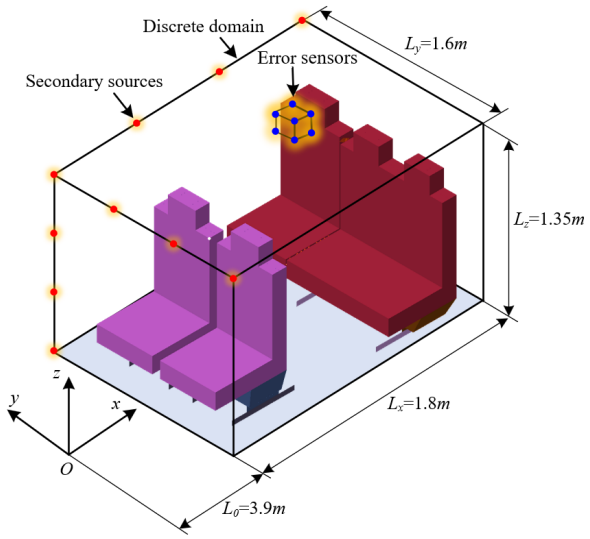

Fig. 2 Schematic diagram of discrete secondary sources and error sensors inside the cabin

As illustrated in Fig. 2, the candidate positions for secondary sources are uniformly distributed within the rectangular cavity. According to engineering requirements, the distance between secondary sources must be smaller than the minimum wavelength of the primary noise. Therefore, the candidate spacing for secondary sources is set to 0.6 *m*. A total of four candidate positions are distributed uniformly along each of the *x*, *y*, and *z* axes, resulting in 64 candidate positions for secondary sources.

Furthermore, nine candidate positions for error sensors are uniformly distributed within a cubic region at the head level of each seat. Given that the helicopter cabin contains five seats, a total of 45 candidate positions are defined for error sensors. In the numerical simulation, each secondary source is sequentially excited with white noise to obtain the acoustic transfer impedance matrix corresponding to the secondary sources.

IV. Optimization Method for Electro-Acoustic Component Placement

Based on the computed acoustic transfer impedance matrices of the control system, the placement optimization of electro-acoustic components in the ANC system is further addressed using the θ-NSGA-III algorithm[8], as illustrated in Fig. 3. The fitness function is defined by Eq.(3), thereby transforming the component placement problem into an optimization task aimed at minimizing $\boldsymbol{J}_e$ through the selection of spatial coordinates for secondary sources and error sensors.

The spatial configuration of electro-acoustic components within the cabin is optimized following the steps below:

Establish a predefined set of reference points. The positions of *N* electro-acoustic components are encoded, with each encoded string $\boldsymbol{E}$ representing an individual in the population. Within the given constraint range, each dimension of the individual is randomly assigned a value to initialize the population. The fitness value $\boldsymbol{F}$ is then computed for each individual and appended to the corresponding encoded string $\boldsymbol{E}$, forming the sequence:

$$\boldsymbol{E}=\begin{bmatrix} l_1 & l_2 & l_3 & \cdots & l_N & F_1 & \cdots \end{bmatrix} \tag{7}$$

To prevent the population from converging to a local optimum, the crossover operation adopts the simulated binary crossover (SBX) method[9]. Let the two randomly selected and distinct parent individuals be denoted as X^1 and X^2; the resulting offspring individual obtained through the crossover operation is denoted as C^1 and C^2.

$$\begin{cases} c_i^1 = 0.5\left[(1+\beta)x_i^1 + (1-\beta)x_i^2\right] \\ c_i^2 = 0.5\left[(1-\beta)x_i^1 + (1+\beta)x_i^2\right] \end{cases} \tag{8}$$

where the crossover factor β is dynamically and randomly determined by the distribution index η.

$$\beta = \begin{cases} (2*r)^{\frac{1}{1+\eta}}, r \le 0.5 \\ \left(\frac{1}{2-2*r}\right)^{\frac{1}{1+\eta}}, r > 0.5 \end{cases} \tag{9}$$

where r denotes a randomly generated number between 0 and 1. The parameter η is user-defined and influences the extent of variation in the offspring; a larger distribution index results in offspring that are closer to their parents. Therefore, the SBX operator performs well in local search optimization and is particularly effective in high-dimensional multi-objective optimization problems.

The mutation operation adopts the polynomial mutation method[10]. The principle is as follows: a randomly selected individual X^t undergoes mutation, and

$$x^t(i) = x^t(i) + \Delta_i, i = 1, 2, \cdots D \tag{10}$$

where

$$\Delta_i = \begin{cases} (2u_i)^{\frac{1}{1+\eta_u}} - 1, u_i < 0.5 \\ 1 - [2(1-u_i)]^{\frac{1}{1+\eta_u}}, u_i \ge 0.5 \end{cases} \tag{11}$$

where u_i is a randomly generated number in the range [0, 1], and η_u is a user-defined non-negative real number.

Combine the parent and offspring populations, and perform adaptive normalization on the objective function values and reference points to ensure comparability across their numerical ranges. Subsequently, a new population is selected for the next iteration using non-dominated sorting based on θ-dominance.

Through the above optimization process, the θ-NSGA-III algorithm effectively optimizes the placement of electro-acoustic components in the cabin ANC system within a high-dimensional objective space, thereby enhancing the noise reduction performance of the ANC system.

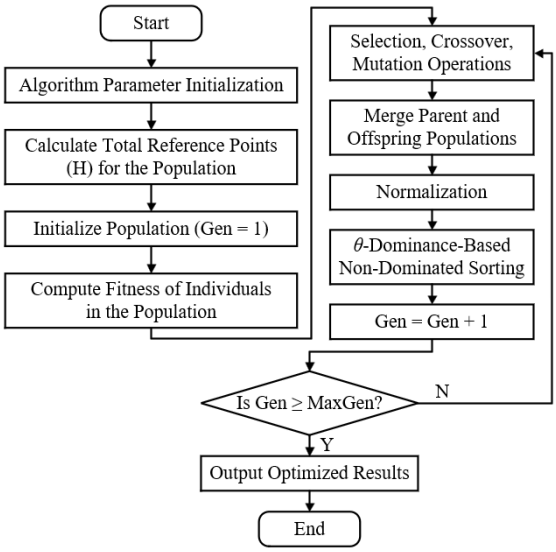

Fig. 3 Flowchart for solving ANC electroacoustic device placement optimization using θ-NSGA-III algorithm

V. THEORETICAL SIMULATION

TABLE 1

SPECIFIC SPATIAL POSITIONS OF ELECTRO-ACOUSTIC COMPONENTS UNDER THE OPTIMAL CONFIGURATION SCHEME.

Electroacoustic device	No.	Position coordinate/m
Secondary sources	1	(4.04, -0.60,0.85)
	2	(4.04, 0.20, 1.02)
	3	(4.87, -0.60, 1.06)
	4	(5.70, 0.60, 0.85)
Error sensors	1	(4.20, -0.375, 1.20)
	2	(4.20, 0.375, 1.20)
	3	(5.30, -0.40, 1.20)
	4	(5.30, 0.35, 1.20)
Reference sensors	1	(3.60, 1.20, 0.80)

TABLE 2

THEORETICAL SIMULATION RESULTS OF NOISE REDUCTION PERFORMANCE UNDER THE OPTIMAL CONFIGURATION SCHEME (20-500Hz).

Position	Noise reduction/dB
Error sensors 1	35.71
Error sensors 2	36.55
Error sensors 3	37.35
Error sensors 4	41.03
Global noise reduction level	37.08

Taking into account both the complexity and feasibility of the noise reduction system—as well as the constraints imposed by the limited internal space and complex geometry of the cabin—the placement positions and quantity of secondary sources are subject to restrictions. Consequently, a 4×4 configuration of secondary sources and error sensors is adopted for the ANC system. The θ-NSGA-III-based optimization algorithm is executed independently multiple times, and the most frequently occurring positions that are also suitable for practical implementation are statistically identified. The results are summarized in TABLE 1. TABLE 2 presents the theoretical simulation results of noise reduction performance under the optimal configuration scheme in the 20–500 Hz frequency range. Analysis of the results indicates that the noise reduction at each of the four error sensors exceeds 35.71 dB, with a global noise reduction reaching 37.08 dB.

VI. EXPERIMENTAL VALIDATION

Based on the optimized configuration of electro-acoustic components, this section further conducts experimental research on active noise control in a helicopter ground simulation cabin. The experimental setup is installed in a semi-anechoic chamber, where the cabin structure is constructed from a square steel frame riveted with aluminum panels. The windshield and cabin door windows are fabricated from acrylic sheets to simulate transparent components, and a sound-absorbing floor panel is installed beneath the cabin to provide structural support.

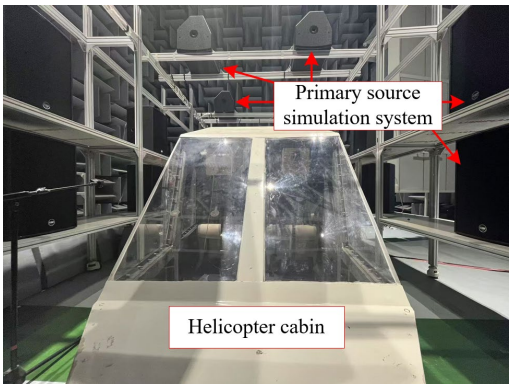

Fig. 4 Helicopter cabin primary source simulation system

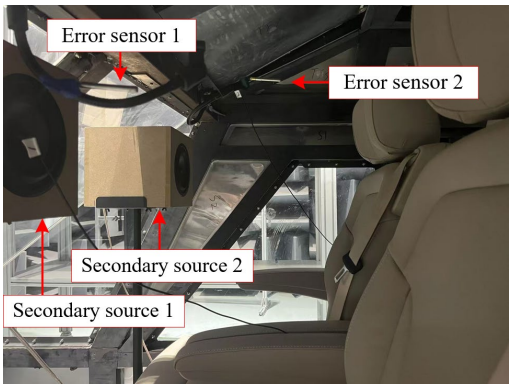

Fig. 5 Schematic diagram of internal layout of the helicopter cabin ANC system

The helicopter noise simulation system consists of 16 loudspeakers (as shown in Fig. 4), along with a power management unit and power amplifiers. The 16 loudspeakers are positioned along the left, right, and top sides of the cabin. Each speaker independently emits a specific noise signal, and together they reproduce the acoustic environment corresponding to actual helicopter operation.

The numerical simulation model used in this paper was constructed at a 1:1 scale with the actual ground-based cabin simulator. Therefore, in the experiment, the placement of electro-acoustic components matches exactly with that used in the computational simulation, as illustrated in Fig. 5. The four secondary loudspeakers are positioned at the optimal locations determined by the optimization algorithm.

During the experiment, the external sound source simulation system of the helicopter mock-up cabin was first activated to generate a background primary noise field inside the cabin. The reference microphone was positioned near the lower row of loudspeakers at the front-right side of the simulated cabin. The control system operated at a sampling rate of 2000 Hz with a 1024-tap filter, and a four-channel Filtered-x Least Mean Square (FxLMS) algorithm was employed to implement active noise control.

Two secondary source placement schemes were designed for comparative testing: (1) the optimal configuration, in which secondary sources and error sensors were arranged according to the algorithm-optimized layout; (2) the conventional configuration, where secondary sources were placed approximately 15 cm from the error sensors.

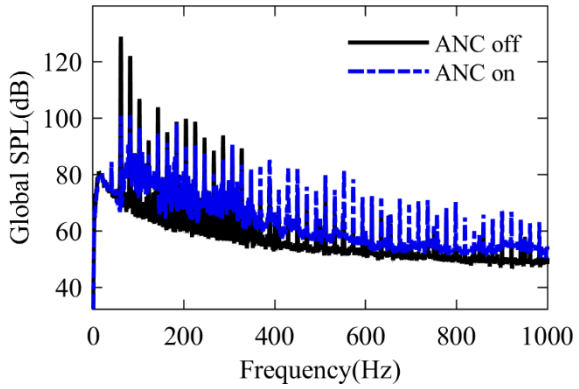

Fig. 6 Global noise spectrum of the helicopter cabin ANC system before and after active control under the optimal configuration

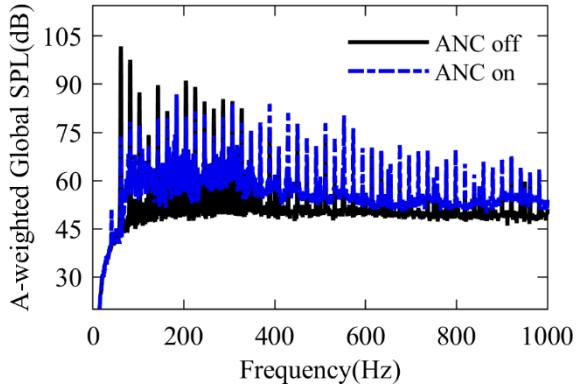

Fig. 7 A-weighted global noise spectrum of the helicopter cabin ANC system before and after active control under the optimal configuration

Fig. 6 and Fig. 7 present the global noise spectrum and A-weighted results of the helicopter cabin ANC system before and after active control under the optimal configuration. As shown, the maximum noise reduction reaches 28.1 dB at 61.5 Hz. Within the 20–500 Hz frequency band, the overall global noise reduction level reaches 21.4 dB, and the A-weighted global noise reduction level is 9.3 dB(A).

TABLE 3
NOISE REDUCTION PERFORMANCE OF THE ANC SYSTEM UNDER DIFFERENT SECONDARY SOURCE CONFIGURATION SCHEMES (20-500Hz).

	Optimal	Conventional
Error sensors 1	19.4 dB	18.4 dB
Error sensors 2	19.1 dB	16.6 dB
Error sensors 3	20.4 dB	19.4 dB
Error sensors 4	22.5 dB	14.2 dB
Global noise reduction level	21.4 dB	16.3 dB

TABLE 3 presents the ANC noise reduction performance of the secondary sources under both the optimal and conventional configurations in the 20–500 Hz frequency range. It can be observed that the optimal configuration achieves superior noise reduction at each error sensor compared to the conventional setup. The global noise reduction under the optimal configuration reaches 21.4 dB, while that of the conventional configuration is only 16.3 dB, indicating that the optimization improves the overall ANC system performance by 5.1 dB. This further validates the effectiveness of the θ-NSGA-III algorithm in optimizing the electro-acoustic layout of helicopter cabin ANC systems.

VII. CONCLUSIONS

This study conducts a multi-objective optimization of the electro-acoustic component layout for helicopter cabin ANC systems based on the θ-NSGA-Ⅲ algorithm. In the theoretical simulation, the acoustic field within the enclosed cabin is spatially discretized, and electro-acoustic components are modeled as point sources, thereby transforming the continuous placement optimization problem into a discrete one. The transfer functions of the control system are obtained through numerical simulation. Taking the minimization of the sum of squared sound pressures near the occupant's head as the optimization objective, multiple independent runs of the θ-NSGA-III algorithm are performed to derive the optimal configuration of electro-acoustic components. A conventional configuration is also defined by placing the secondary sources approximately 15 *cm* from the head-level error sensors. Comparative experimental validation of both configurations shows that the optimal layout achieves a 5.1 dB improvement in global noise reduction over the conventional setup, thereby demonstrating the effectiveness of the proposed optimization method.

REFERENCES

[1] J. Caillet, F. Marrot, Y. Unia, P.-A. Aubourg, Comprehensive approach for noise reduction in helicopter cabins, Publisher, City, 2012.

[2] F. Ernst, D. Sachau, Cabin noise analysis of an H120 B helicopter for active noise control applications, in, Institute of Noise Control Engineering, pp. 1761-1771.

[3] Y. Yuan, H. Xu, B. Wang, An improved NSGA-III procedure for evolutionary many-objective optimization, in, pp. 661-668.

[4] Y. Wang, T. Zhao, Y. Chen, L. Zou, L. Zhang, T. Yang, Comprehensive Optimization Strategy of Secondary Sound Source in Active Noise Control System of Power Transformer Based on Monte Carlo Method, in, IEEE, pp. 1128-1133.

[5] Y. Huang, H. Zhang, K. Zhao, E. Xu, Q. Huang, J. Wang, Precise Configuring of Actuators/Sensors for Active Control of Sound Quality in Cabs with Modal Vibration Energy and LA-PSO, Publisher, City, 2023.

[6] K.H. Baek, S.J. Elliott, Natural algorithms for choosing source locations in active control systems, Publisher, City, 1995.

[7] X. Wang, L. Zhang, Q. Li, J. Lou, X. Sun, Parameter optimization analysis of the secondary acoustic sources for power transformer active noise control, Publisher, City, 2012.

[8] K. Deb, H. Jain, An evolutionary many-objective optimization algorithm using reference-point-based nondominated sorting approach, part I: solving problems with box constraints, Publisher, City, 2013.

[9] L. Kong, J. Wang, P. Zhao, Solving the dynamic weapon target assignment problem by an improved multiobjective particle swarm optimization algorithm, Publisher, City, 2021.

[10] D. Jung, Y.H. Choi, J.H. Kim, Multiobjective automatic parameter calibration of a hydrological model, Publisher, City, 2017.